



ARTICLE

Combinations of proteasome inhibitors with obatoclox are effective for small cell lung cancer

Yan-ping Yin^{1,2,3}, Wen-hao Shi⁴, Ke Deng^{1,2,3}, Xiao-li Liu^{1,2,3}, Hong Li^{1,3}, Xiao-tong Lv^{1,2,3}, Vivian Wai Yan Lui⁵, Chen Ding^{6,7,8}, Bo Hong^{1,3} and Wen-chu Lin^{1,3}

Proteasome inhibitors, bortezomib (BTZ), and carfilzomib (CFZ) are approved drugs for hematological malignancies, but lack anticancer activities against most solid tumors. Small cell lung cancer (SCLC) is a very aggressive neuroendocrine carcinoma of the lungs demanding effective therapy. In this study we investigated whether BTZ or CFZ combined with obatoclox (OBX), an antagonist for MCL-1 and a pan-BCL family inhibitor, could cause synergistic growth inhibition of SCLC cells. We showed that combined application of BTZ or CFZ with OBX caused synergistic growth inhibition of human SCLC cell lines (H82, H526, DMS79, H196, H1963, and H69) than single agent alone. Both BTZ–OBX and CFZ–OBX combinations displayed marked synergism on inducing apoptosis (~50% increase vs BTZ or CFZ alone). A comprehensive proteomics analysis revealed that BTZ preferentially induced the expression of MCL-1, an antiapoptotic protein, in SCLC cells. Thus, proteasome inhibitor–OBX combinations could specifically induce massive growth inhibition and apoptosis in SCLC cells. Subsequent proteome-wide profiling analysis of activated transcription factors suggested that BTZ- or CFZ-induced MCL-1 upregulation was transcriptionally driven by FOXM1. In nude mice bearing in SCLC H82 xenografts, both BTZ–OBX, and CFZ–OBX combinations exhibited remarkable antitumor activities against SCLC tumors evidenced by significant reduction of tumor size and the proliferation marker Ki-67 signals in tumor tissues as compared with single agent alone. Thus, proteasome inhibitor–OBX combinations are worth immediate assessments for SCLC in clinical settings.

Keywords: small cell lung cancer; obatoclox; bortezomib; carfilzomib; MCL-1; apoptosis; FOXM1; proteomics analysis

Acta Pharmacologica Sinica (2021) 42:1298–1310; <https://doi.org/10.1038/s41401-020-00544-w>

INTRODUCTION

Cancer cells are known to exert heavy demands on proteasome function to support their increased rate of protein production and turnover due to their rapid rates of cell division. Such a high level of proteasomal dependency can be potentially targeted by proteasome inhibitors to curb the growth of cancer cells [1, 2]. Bortezomib (BTZ) and carfilzomib (CFZ) are two FDA-approved proteasome inhibitors for the treatment of hematological malignancies. However, their clinical activities have been shown to be moderate or limited in many other solid tumors [3–5]. BTZ is reversible, while CFZ is an irreversible proteasome inhibitor. CFZ shows superior clinical efficacy and fewer adverse effects than BTZ [6, 7].

Small cell lung cancer (SCLC), a very aggressive lung cancer of neuroendocrine origin, represents ~15% of all lung cancer cases [8]. Platinum-based chemotherapy (cisplatin and carboplatin) combined with the topoisomerase inhibitor etoposide is a standard SCLC treatment regimen. Despite good initial responses to chemotherapy, recurrence, and resistance inevitably occur in almost all SCLC patients [9]. Currently, SCLC patients have a dismal

median progression-free survival of less than 5 months [10]. Thus, there is an urgent demand to develop more effective therapeutic strategies for SCLC.

BTZ and CFZ have been clinically investigated in SCLC patients in the past, as well as recently [11–13]. In a BTZ clinical trial on 56 relapsed or refractory SCLC patients, limited clinical activity was observed for most patients, except for one patient with platinum-refractory SCLC, who demonstrated a partial response [11]. Similarly, in a phase I clinical trial of the CFZ–irinotecan combination, the treatment was well tolerated by SCLC patients. However, only one patient (out of 13 total) demonstrated a partial response [12]. Though proteasome inhibitors seem to be well tolerated in SCLC patients, these single agents are definitely suboptimal in inhibiting SCLC growth or progression.

The reasons underlying the limited antitumor activities of BTZ or CFZ in SCLC are likely complex. Here, by a comprehensive proteomics analysis, we first indicated that MCL-1, an antiapoptotic protein, was preferentially induced by BTZ (vs CFZ) in SCLC cells, and such MCL-1 upregulation may potentially limit the

¹High Magnetic Field Laboratory, Chinese Academy of Sciences, Hefei 230031, China; ²University of Science and Technology of China, Hefei 230036, China; ³Key Laboratory of High Magnetic Field and Ion Beam Physical Biology, Hefei Institutes of Physical Science, Chinese Academy of Sciences, Hefei 230031, China; ⁴State Key Laboratory of Proteomics, Beijing Proteome Research Center, Beijing Institute of Lifeomics, National Center for Protein Sciences (The PHOENIX Center, Beijing), Beijing 102206, China; ⁵School of Biomedical Sciences, Faculty of Medicine, The Chinese University of Hong Kong, Hong Kong, Hong Kong SAR, China; ⁶State Key Laboratory of Genetic Engineering, Human Phenome Institute, Institutes of Biomedical Sciences, School of Life Sciences, Zhongshan Hospital, Fudan University, Shanghai 200433, China; ⁷State Key Laboratory of Cell Differentiation and Regulation, College of Life Science, Henan Normal University, Xinxiang 453007, China and ⁸Academy of Medical Science, Zhengzhou University, Zhengzhou 450052, China
Correspondence: Chen Ding (chend@fudan.edu.cn) or Bo Hong (bhong@hmfl.ac.cn) or Wen-chu Lin (wenchu@hmfl.ac.cn)

These authors contributed equally: Yan-ping Yin, Wen-hao Shi

Received: 19 May 2020 Accepted: 18 September 2020

Published online: 2 November 2020

clinical efficacies of BTZ and CFZ in SCLC. Most strikingly, either BTZ or CFZ, when combined with obatoclax (OBX), an antagonist for MCL-1, could cause the synergistic growth inhibition and apoptosis of SCLC cells compared with single agents alone, and the combinations resulted in the concomitant reduction of MCL-1 expression. Subsequent proteome-wide profiling analysis of activated transcription factors (TFs) suggested that BTZ- or CFZ-induced MCL-1 upregulation was transcriptionally driven by FOXM1. Strikingly, *in vivo* investigations first demonstrated novel and remarkable antitumor activities of both the BTZ–OBX and CFZ–OBX combinations against SCLC tumors.

MATERIALS AND METHODS

Materials

BTZ and CFZ were purchased from Selleck Chemical (Shanghai, China). OBX and cycloheximide (CHX) were purchased from MCE (Concord, CA, USA). Antibodies against PARP, cleaved-caspase 3, MCL-1, FOXM1, and HIF-1 α were purchased from Cell Signaling Technology (Danvers, MA, USA). β -Actin antibody was purchased from TransBionovo (Beijing, China).

Cell line maintenance

The human SCLC cell lines H82, H526, DMS79, H196, H1963, and H69 were maintained in RPMI-1640 media supplemented with 10% fetal bovine serum and 1% penicillin/streptomycin (Gibco, Life Technologies, Carlsbad, CA, USA) in an incubator at 37 °C with 5% CO₂.

Protein extraction and trypsin digestion

H82 cells were treated with DMSO vehicle control or 10 nM BTZ or CFZ for 24 h in triplicate. The treated cells were collected and washed with cold 1x PBS. The cell pellets were then lysed in lysis buffer containing 1% sodium deoxycholate, 10 mM Tris (2-carboxyethyl) phosphine, 40 mM 2-chloroacetamide, and 100 mM Tris (pH 8.5). After vortexing and heating at 95 °C for 5 min, the cell lysates were ultrasonicated by a handheld ultrasound device for 5 min. The lysates were then centrifuged at 16,000 $\times g$ for 10 min, and the supernatants were collected for protein quantification. A total of 50 μg of protein was treated with trypsin at a ratio of 50:1 (protein:trypsin). Digestion in solution was performed at 37 °C for 4 h. Formic acid was then added to a final concentration of 1% to precipitate the proteins, followed by centrifugation at 16,000 $\times g$ for 10 min. The supernatant was desalted by a homemade C18 tip.

The enrichment of TFs with transcription factor response elements (TFREs)

The nuclear extracts of the treated cells were extracted according to the manufacturer's instructions (Thermo Fisher Scientific, Catalog number: 78835), and 100 μg of nuclear extract was used for TF enrichment. Twenty microliters of Dynabeads M280 streptavidin (Invitrogen, Catalog number: 00324960) with 0.5 pmol TFRE DNA was used for TF enrichment for each sample. The protein–DNA complexes were digested with trypsin and analyzed with mass spectrometry. The detailed procedure was described previously [14, 15].

Liquid chromatography–tandem mass spectrometry (LC–MS/MS) analysis

Dried peptide samples were dissolved in solvent A (0.1% formic acid in water). For whole proteomic profiling, LC–MS/MS analysis was performed with an Orbitrap Fusion mass spectrometer (Thermo Fisher Scientific, USA) equipped with the online Easy-nLC 1000 nano-HPLC system (Thermo Fisher Scientific, USA). The injected peptides were separated on a reverse-phase nano-HPLC C18 column (precolumn, 3 μm , 120 Å , 2 cm \times 100 μm i.d.; analytical column, 1.9 μm , 120 Å , 30 cm \times 150 μm i.d.) with a

150-min gradient of 5%–40% solvent B (0.1% formic acid in acetonitrile).

For TF activity samples, a Q Exactive HF mass spectrometer equipped with the online Easy-nLC 1200 nano-HPLC system (Thermo Fisher Scientific, USA) was used. The injected peptides were separated on a reverse-phase nano-HPLC C18 column (precolumn, 3 μm , 120 Å , 2 cm \times 100 μm i.d.; analytical column, 1.9 μm , 120 Å , 12 cm \times 150 μm i.d.) with a 75-min gradient of 6%–42% solvent B (0.1% formic acid in 80% acetonitrile).

Data processing

The acquired MS/MS spectra were searched by Mascot 2.3 (Matrix Science Inc.) implemented on Firmiana [16] against the human National Center for Biotechnology Information RefSeq protein databases (updated on April 7, 2013, 32 015 protein entries). The parameter settings were as follows: mass tolerances of 20 ppm for precursor ions and 0.5 Da (Orbitrap Fusion) or 0.05 Da (Q Exactive HF) for product ions; database searches were performed with trypsin (K/R) specificity, and two missed cleavage sites were allowed. Label-free quantification was used. For the whole proteomic profiling data, dynamic modifications included acetyl (protein N-term) and oxidation (M), and the fixed modification was carbamidomethyl (C). Dynamic modifications for TF activity data were phospho (Y), phospho (ST), acetyl (protein N-term), and oxidation (M). A false discovery rate of 1% was applied for protein inference.

FOT data were used to select protein changes. Proteins with a unique strict peptide number greater than 0 in at least one sample and detected more than two times in three biological repeat samples in at least one treatment group were selected. A 3-fold change in average was selected as the judgement standard of significantly changed proteins. The TF activity change was based on the fold change and *t* test. The raw data were deposited to iProX (<http://www.iprox.org/index>) with the data set identifier project ID IPX0001390000.

Cell viability assay

SCLC cells were seeded in a 96-well white plate (Costar, Kennebunk, ME, USA) at 3000 cells/well. The cells were treated with vehicle control or the drugs for 72 h in triplicate. Relative cell viability was determined by the CellTiter-Glo Luminescent assay (Promega, Madison, WI, USA). The luminescent signals were measured by a multilabel plate reader (Envision PerkinElmer, USA).

Western blotting

After treatment, cell lysates were collected for Western blotting as previously described [17]. Twenty micrograms of protein was used for SDS-polyacrylamide gel electrophoresis. After primary and secondary antibody incubation, the signals were detected by ECL Western blotting substrate (Thermo Fisher Scientific, USA). β -Actin was used as the loading control.

Detection of MCL-1 degradation

Protein degradation in SCLC cells was determined by Western blotting following CHX treatment for various time points. SCLC cells were treated with 12 nM BTZ (24 nM CFZ) with or without 50 $\mu g/mL$ CHX at different time points (0, 0.5, 1, 2, 3, and 4 h). The cells were then lysed for MCL-1 expression detection by Western blotting. β -Actin was used as a loading control.

Quantitative real-time RT-PCR

The cellular RNA of the treated cells was extracted using the RNeasy Mini RNA Kit (Qiagen, Hilden, Germany). Complementary DNA was synthesized using the Transcriptor First Strand cDNA Synthesis Kit (Roche, Mannheim, Germany) according to the manufacturer's instructions. Quantitative real-time PCR was performed in triplicate using FastStart Essential DNA Green Master Mix (Roche, Mannheim, Germany) on the Roche LightCycler 96

Real-Time PCR System. The mRNA expression level of the MCL-1 gene was normalized to the expression level of β -Actin. The primers for MCL-1 and β -Actin were as follows:

β -Actin

Forward 5'-CATGTACGTTGCTATCCAGGC-3',

Reverse 5'-CTCCTTAATGTCACGCACGAT-3';

MCL-1

Forward 5'-AAGCCAATGGGCAGGTCT-3',

Reverse 5'-TGTCAGTTCCGAAGCAT-3'.

Annexin V apoptosis analysis

After treatment, cells were collected and then stained with FITC Annexin V and PI using a FITC Annexin V Apoptosis Detection Kit (BD Pharmingen, San Diego, CA, USA). The stained cells were subjected to flow cytometry analysis by FACSCalibur (BD Pharmingen, San Diego, CA, USA). Then, the results were analyzed using FlowJo software (BD Pharmingen, Ashland, Oregon, USA).

Generation of SCLC cells with stable FOXM1 knockdown

FOXM1 shRNA was cloned into the pLKO.1 vector. The FOXM1 shRNA-expressing vector and lentivector packaging plasmids psPAX2 and pMD2.G were cotransfected into HEK-293T cells using Effectene Transfection Reagent (QIAGEN, Hilden, Germany) for 6–8 h, which was then replaced with fresh medium. Viral supernatant was harvested 48 h after transfection.

SCLC H196 cells were infected with lentiviral particles in the presence of 8 μ g/mL polybrene (Sigma-Aldrich, Steinheim, Germany) for 24 h, followed by growth in fresh medium for 24 h. Then, puromycin (Solarbio, Beijing, China) at 1 μ g/mL was added for selection. After 14 days of selection, puromycin-resistant cells were collected for FOXM1 knockdown validation by Western blotting.

Chromatin immunoprecipitation (ChIP) assays

H82 cells were treated with DMSO, BTZ (12 nM), and CFZ (48 nM) for 24 h. The cells were fixed for 10 min with 1% formaldehyde and then lysed in lysis buffer (1% SDS, 10 mM EDTA, 50 mM Tris-HCl pH 8.0 plus proteasome inhibitor). The chromatin was sonicated to shear the DNA to an average length between 100 and 1000 bp. Then, the chromatin was immunoprecipitated with FOXM1 antibodies (2.5 μ g) and with equal amounts of immunoglobulin G (IgG) as negative controls. qPCR was performed in triplicate by amplifying 50 ng of immunoprecipitated chromatin DNA with gene-specific primers. Primer pairs were designed against the FOXM1-binding element (FBE2, -728 to -582) of the MCL-1 promoter region [18]. Primer pairs were also designed against the promoter region of β -Actin as a negative control [19].

Combination index (CI) determination

Drug synergy was quantitatively assessed using the CI method of Chou and Talalay [20]. The CI was calculated using CalcuSyn software (Biosoft, Cambridge, UK). CI < 1 indicates synergism, whereas CI > 1 indicates antagonism.

Xenograft experiments

Animal experiments were carried out according to a protocol approved by the Institutional Animal Care and Use Committee of Hefei Institutes of Physical Science, China. Athymic nude mice were subjected to subcutaneous tumor inoculation at the dorsal flank, with a 100 μ L suspension of 2×10^6 H82 cells in an equal volume of Matrigel (BD Biosciences, Franklin, NJ, USA). When tumors grew to 4–5 mm in diameter, the mice were randomized into six different groups. The mice were intraperitoneally injected with either DMSO control, BTZ (2 mg/kg), CFZ (2 mg/kg), OBX (3 mg/kg), the combination of BTZ/OBX or the combination of CFZ/OBX every 3 days. The tumor size was monitored by caliper measurements and calculated by the following formula: Volume = (length \times width \times width)/2.

H&E staining and immunohistochemistry were performed as previously described [21]. The expression of Ki-67 and cleaved-caspase 3 was quantified by ImageJ (NIH, USA).

Statistical analysis

All data were analyzed using Prism 5 Software (GraphPad Software, Inc., La Jolla, CA, USA). Statistical analysis was performed using an unpaired *t* test. The results were considered statistically significant when *P* < 0.05.

RESULTS

Preferential induction of MCL-1 with BTZ treatment in SCLC cells. First, we assessed the antitumor activities of BTZ and CFZ in SCLC cell lines (H82, H526, DMS79, H1963, H196, and H69). Cell proliferation assays showed that the IC₅₀ values of CFZ were lower than those of BTZ in these SCLC cell lines, indicating that the in vitro anti-SCLC activity of CFZ was superior to that of BTZ (Fig. 1a). We sought to determine the effects of BTZ and CFZ treatments on SCLC cells by proteomics to provide potential ways to improve proteasome inhibitor treatment regimens in SCLC. SCLC cells were more sensitive to CFZ than BTZ, which implied that some proteins preferentially induced by BTZ (vs CFZ) may limit the antitumor activities of BTZ and CFZ. Therefore, proteomic profiling data were screened to rank the proteins, which were induced by BTZ treatment with >3-fold changes and by CFZ treatment with 1- to 3-fold changes. As shown in Fig. 1b and Supplementary Table 1, proteomics analysis found that BTZ treatment of SCLC H82 cells resulted in the upregulation of proteins related to G₂/M cell cycle arrest and DNA damage repair. Among these proteins, a known antiapoptotic protein, MCL-1, was also found to be induced by BTZ (20-fold upregulation) and CFZ (1.6-fold upregulation). This finding was subsequently confirmed by Western blotting in H82 cells and H526 cells (Fig. 1c). Consistent with the proteomics data, the lower dose (12 nM) of BTZ treatment dramatically induced MCL-1 expression in both the H82 and H526 SCLC cell lines, while the higher dose (24 or 48 nM) of CFZ treatment dramatically upregulated the expression of MCL-1. It is possible that MCL-1, or potentially other antiapoptotic proteins, may at least partially contribute to the limited efficacy of BTZ and CFZ treatments in SCLC.

Synergistic growth inhibition of various SCLC cells by BTZ–OBX. OBX, an antagonist for MCL-1 and a pan-BCL family inhibitor, has been tested in SCLC clinical trials and has shown well-tolerated toxicity but with limited clinical efficacy [22, 23]. Based on our proteomic findings, we attempted to use OBX to determine whether it can effectively increase the anticancer activity of BTZ in SCLC. To test this hypothesis, we calculated the CI of BTZ/OBX cotreatment in SCLC cells (Fig. 2a). The data demonstrated that the BTZ/OBX combination had low CI values (<1) in SCLC cells, indicating that the BTZ/OBX combination exhibited a good synergistic anti-SCLC effect. To indicate that the observed synergistic antitumor effect was MCL-1 specific, H82 and H526 cells were treated with BTZ combined with ABT-263, which only inhibited BCL-2 and BCL-X_L but not MCL-1. Cell viability assays indicated that no synergistic antitumor effect was observed when ABT-263 was combined with BTZ in H82 and H526 cells (Supplementary Fig. 1). Interestingly, we found that when OBX was cotreated with BTZ in SCLC cells, the induction of MCL-1 by BTZ was dramatically decreased (Fig. 2b). Thus, we first demonstrated that BTZ, when combined with an inducer of apoptosis, can exert remarkable growth inhibition in multiple SCLC models.

Synergistic growth inhibition of SCLC cells by CFZ–OBX

MCL-1 is also moderately induced by CFZ. Next, we sought to determine whether this synergistic activity on SCLC cell growth inhibition was observed for the CFZ and OBX combination. As shown in Fig. 3a, the CFZ/OBX combination had low CI values (<1)

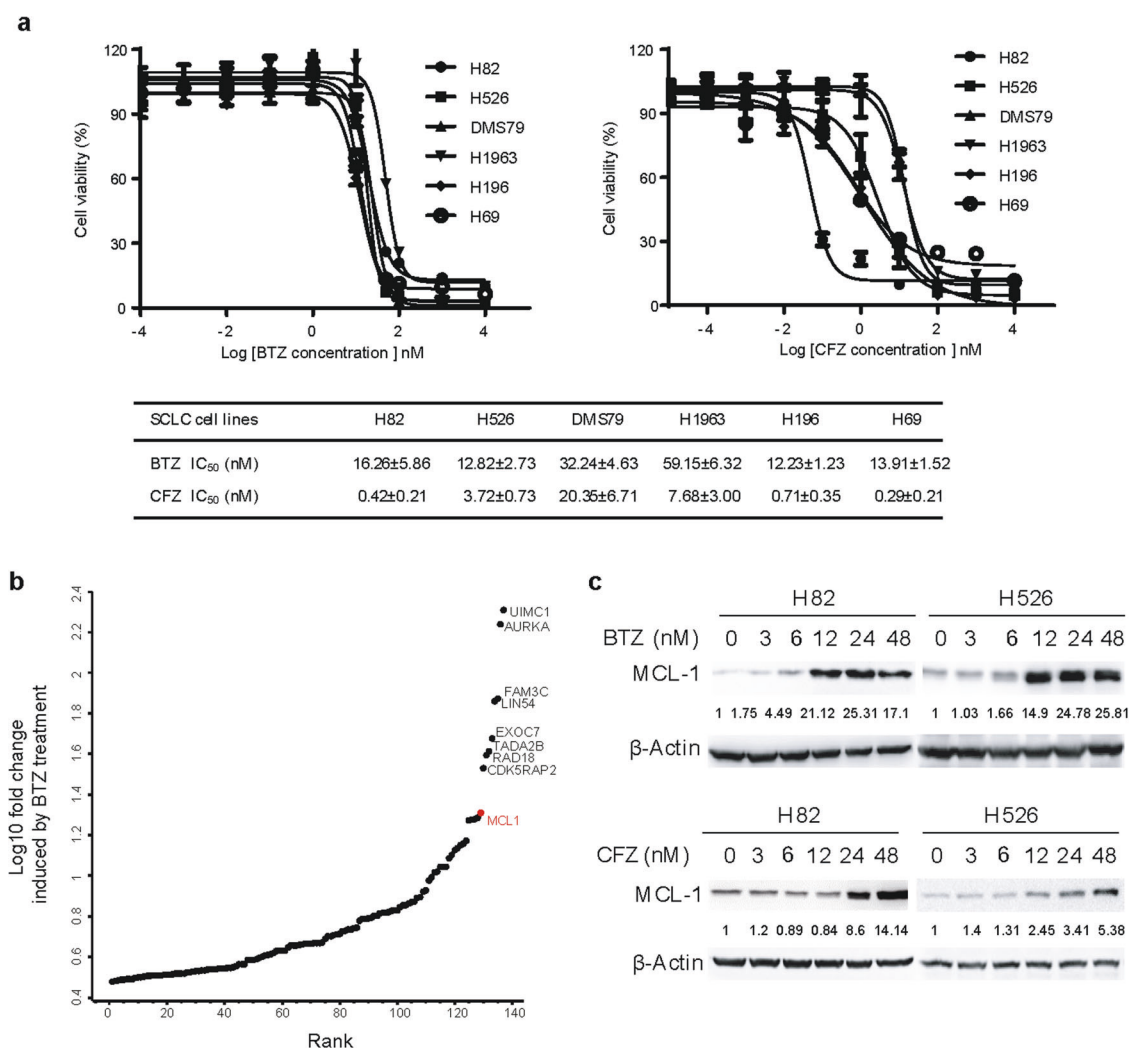


Fig. 1 BTZ treatment preferentially induced MCL-1 expression in SCLC cells. **a** Growth inhibition curves of BTZ and CFZ in a panel of SCLC cell lines. Various SCLC cell lines were treated with different concentrations (10^{-3} nM– 10μ M) of CFZ and BTZ for 72 h. Cell viability was assessed by the CellTiter-Glo assay. The IC₅₀ values were determined from the sigmoidal dose-response curves using Prism 5 software. **b** Proteomic analysis indicated that MCL-1 was preferentially induced by BTZ treatment. By screening proteomics data, proteins induced by BTZ treatment with >3-fold changes and by CFZ treatment with 1- to 3-fold changes were ranked. **c** Validation of MCL-1 upregulation by BTZ/CFZ treatment in SCLC cells by Western blotting. SCLC cells (H82 and H526 cells) were treated with DMSO control or different doses of BTZ/CFZ for 24 h. After treatment, MCL-1 was detected by Western blotting. β -Actin was used as a loading control. The density of the bands was quantified and normalized to the respective β -Actin band intensity.

in SCLC cells, indicating that the CFZ/OBX combination exhibited a synergistic anti-SCLC effect. Compared with the CFZ/OBX combination treatment, the BTZ/OBX combination had lower CI values in SCLC cells, indicating that the BTZ/OBX combination exhibited a better synergistic anti-SCLC effect. The better synergism of BTZ/OBX was likely due to the stronger induction of MCL-1 by BTZ than CFZ. Similarly, to indicate that the observed synergistic antitumor effect was MCL-1 specific, H82 and H526 cells were also treated with CFZ combined with ABT-263. Cell viability assays indicated that no synergistic antitumor effect was observed when ABT-263 was combined with CFZ in H82 and H526 cells (Supplementary Fig. 2). Furthermore, the induction of MCL-1 by CFZ was dramatically decreased by the OBX combination (Fig. 3b). Thus, we first demonstrated that CFZ, when combined with OBX, could also remarkably inhibit SCLC growth.

Synergistic apoptosis induced by both the BTZ–OBX and CFZ–OBX combinations

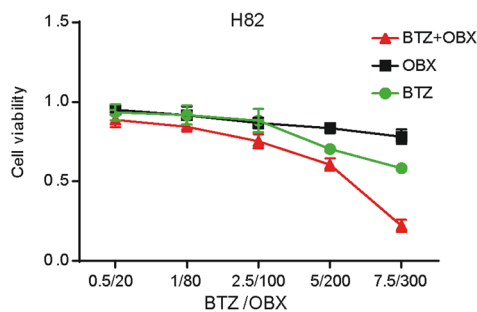
Since OBX is a known inducer of apoptosis, we examined the effects of both BTZ–OBX and CFZ–OBX on apoptosis by flow

cytometry and PARP cleavage (vs each of the single agents alone). As shown in Fig. 4a, we found that in H82 cells, both the BTZ–OBX and CFZ–OBX combinations could cause marked synergism on apoptosis. Increases as high as ~50% were observed in both combinations compared to BTZ or CFZ alone. Furthermore, Western blotting indicated that the cotreatment of BTZ or CFZ with OBX induced more PARP cleavage (apoptotic marker) in SCLC (Fig. 4b). Thus, we first demonstrated that BTZ or CFZ, when combined with OBX, could also remarkably induce SCLC apoptosis.

BTZ- and CFZ-induced MCL-1 transcription through FOXM1 upregulation

We subsequently investigated the potential mechanism contributing to such an increase in MCL-1, which appeared to impede the anticancer activity of BTZ (or CFZ) in SCLC cells. MCL-1 is a short half-life protein, and its expression is tightly regulated by proteasome-mediated degradation [24]. Therefore, we examined whether BTZ- and CFZ-induced MCL-1 expression by inhibiting its degradation. After H82 and H526 cells were treated with CHX

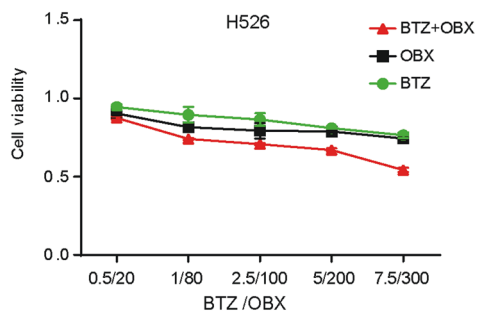
a



Combination index (CI) of BTZ and OBX in H82 cells

BTZ (nM)	OBX (nM)	Fa	CI
0.5	20	0.11241	0.615
1	40	0.155824	0.738
2.5	100	0.246639	0.862
5	200	0.393831	0.71
7.5	300	0.778987	0.131

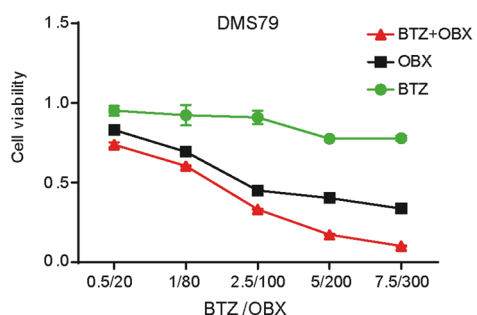
Fa: the fraction of cell death



Combination index (CI) of BTZ and OBX in H526 cells

BTZ (nM)	OBX (nM)	Fa	CI
0.5	20	0.124865	1.06
1	40	0.25808	0.24
2.5	100	0.291576	0.407
5	200	0.329211	0.546
7.5	300	0.45641	0.254

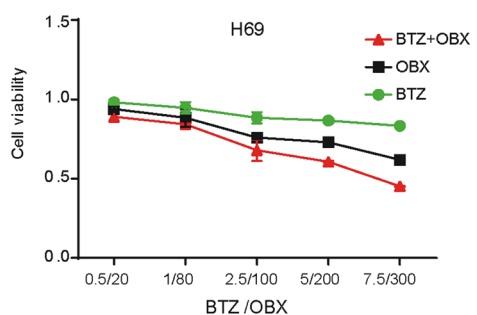
Fa: the fraction of cell death



Combination index (CI) of BTZ and OBX in DMS79 cells

BTZ (nM)	OBX (nM)	Fa	CI
0.5	20	0.261947	0.664
1	40	0.39577	0.626
2.5	100	0.66816	0.397
5	200	0.826883	0.277
7.5	300	0.898244	0.197

Fa: the fraction of cell death



Combination index (CI) of BTZ and OBX in H69 cells

BTZ (nM)	OBX (nM)	Fa	CI
0.5	20	0.1088	0.656
1	40	0.15714	0.774
2.5	100	0.320816	0.607
5	200	0.392585	0.822
7.5	300	0.548396	0.562

Fa: the fraction of cell death

b

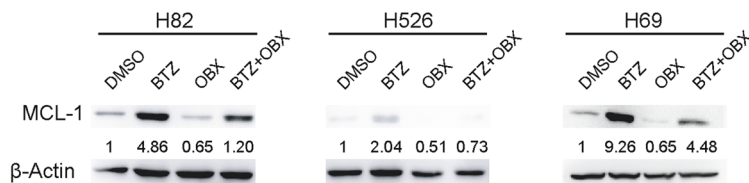


Fig. 2 The BTZ–OBX combination caused synergistic growth inhibition in SCLC cells. **a** CI of BTZ and OBX cotreatment in SCLC cells (H82, H526, DMS79, and H69 cells). **b** Western blotting indicates that BTZ and OBX cotreatment dramatically decreases MCL-1. SCLC cells (H82, H526, and H69 cells) were treated with DMSO control, BTZ (12 nM), OBX (200 nM), or BTZ plus OBX for 24 h. MCL-1 was detected by Western blotting. β-Actin was used as a loading control. The density of the bands was quantified and normalized to the respective β-Actin band intensity.

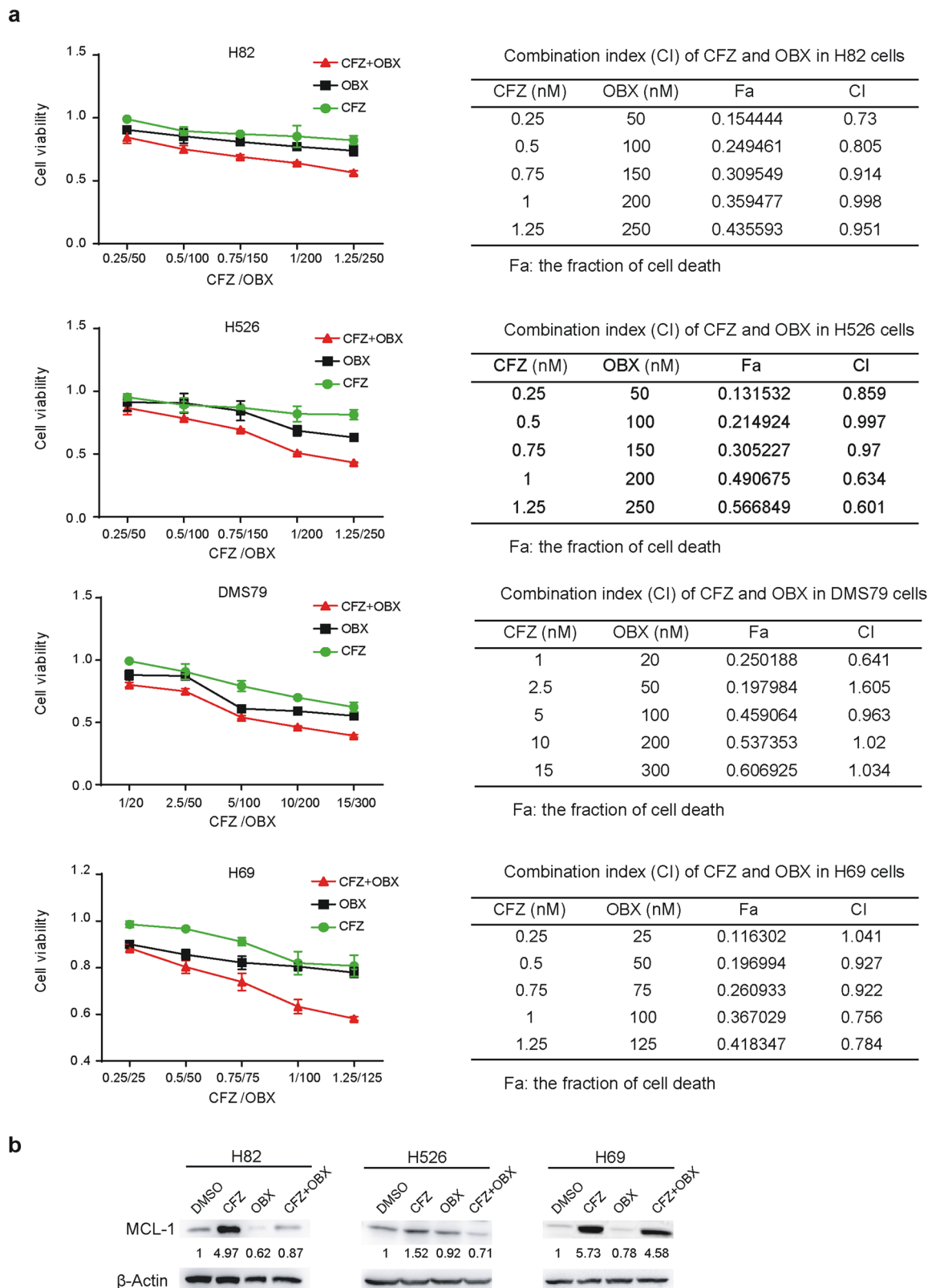


Fig. 3 The CFZ–OBX combination caused synergistic growth inhibition in SCLC cells. **a** CI of CFZ and OBX cotreatment in SCLC cells (H82, H526, DMS79, and H69 cells). **b** Western blotting indicates that CFZ and OBX cotreatment dramatically decreases MCL-1. SCLC cells (H82, H526, and H69 cells) were treated with DMSO control, CFZ (24 nM), OBX (200 nM), or CFZ plus OBX for 24 h. MCL-1 was detected by Western blotting. β -Actin was used as a loading control. The density of the bands was quantified and normalized to the respective β -Actin band intensity.

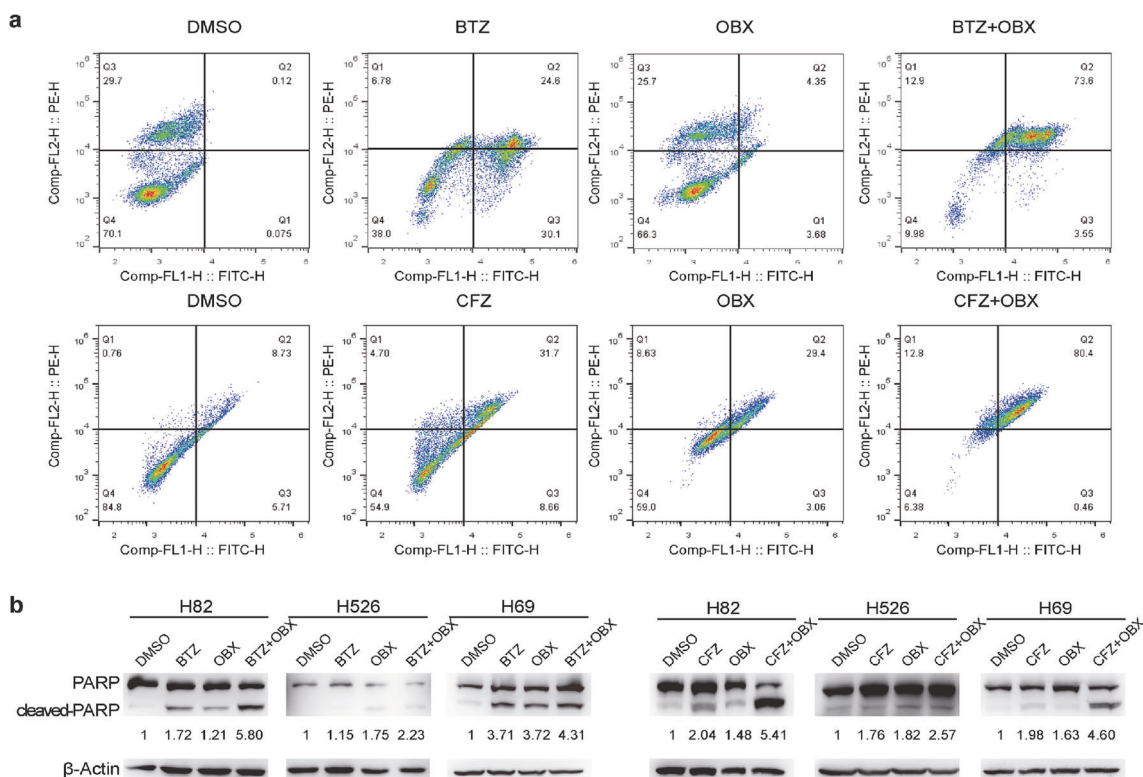


Fig. 4 The BTZ–OBX and CFZ–OBX combinations induced synergistic apoptosis. **a** BTZ/CFZ and OBX cotreatment dramatically induced apoptosis as indicated by Annexin V staining. H82 cells were treated with DMSO control, BTZ (12 nM), CFZ (3 nM), OBX (200 nM), or the combination of BTZ or CFZ and OBX for 24 h. After treatment, an Annexin V apoptotic assay was performed by flow cytometry. The percentage of apoptotic cells (Annexin V positive) is shown in regions Q2 and Q3. **b** Western blotting indicates that BTZ/CFZ and OBX cotreatment induces PARP cleavage. SCLC cells (H82, H526, and H69 cells) were treated with DMSO control, BTZ (12 nM), CFZ (24 nM), OBX (200 nM), or BTZ/CFZ plus OBX for 24 h. PARP and cleaved PARP were detected by Western blotting. β-Actin was used as a loading control. The density of the bands was quantified and normalized to the respective β-Actin band intensity.

(a eukaryote protein synthesis inhibitor) alone or together with BTZ and CFZ, Western blotting showed that the degradation of MCL-1 was not inhibited by BTZ and CFZ treatment (Fig. 5a). Next, we examined whether BTZ- and CFZ-induced MCL-1 mRNA expression. Quantitative RT-PCR indicated that BTZ and CFZ treatment increased MCL-1 mRNA levels in H82 and H526 cells (Fig. 5b), which was consistent with the protein levels induced by BTZ and CFZ treatment (Fig. 1c).

We hypothesized that BTZ and CFZ treatment upregulated the expression of transcriptional factors that induced MCL-1 transcription. Thus, we performed a proteome-wide profiling analysis of activated TFs enriched with TFRES. In the BTZ treatment set, HIF-1α and FOXM1 were labeled in upregulated TFs because they were reported to induce MCL-1 transcription [18, 25, 26] (Fig. 6a). As shown in Fig. 6b, we performed Western blotting experiments and found that HIF-1α and FOXM1 were preferentially induced upon BTZ treatment compared with CFZ treatment. We thus examined whether these two TFs could mediate MCL-1 upregulation in SCLC cells. Specific siRNA knockdown of HIF-1α did not alter MCL-1 levels upon BTZ (12 nM) or CFZ (48 nM) treatment (Supplementary Fig. 3), while FOXM1 shRNA abrogated BTZ (12 nM) or CFZ (48 nM)-induced MCL-1 expression in SCLC cells (Fig. 7a). We then tested whether FOXM1 knockdown enhanced the antitumor activity of BTZ or CFZ. Cell viability assays indicated that the inhibition of cell growth by BTZ or CFZ was significantly enhanced when FOXM1 was knocked down in H196 cells (Fig. 7b). As shown in Fig. 7c, upon FOXM1 knockdown in H196 cells, the cellular apoptosis induced by BTZ or CFZ was also increased (Control vs FOXM1 KD: 35.6% vs. 64.2% for BTZ treatment and 47.1% vs.

75.3% for CFZ treatment). To further investigate whether FOXM1 binds to the MCL-1 promoter, we performed ChIP assays with H82 cells treated with DMSO, BTZ, or CFZ. The qPCR results showed that FOXM1 induced by BTZ or CFZ treatment was specifically enriched in the promoter region of MCL-1 in H82 SCLC cells (Fig. 7d). These data indicate that BTZ and CFZ induce the transcription of MCL-1 by FOXM1 upregulation in SCLC.

The BTZ–OBX and CFZ–OBX combinations exhibited significant antitumor activities in vivo
Next, we determined the in vivo antitumor efficacies of both combinations in an SCLC model. Mice were subcutaneously inoculated with H82 SCLC cells (100 million per tumor). When the tumor size reached 4–5 mm in diameter, the mice were randomized into six groups for vehicle alone, 2 mg/kg BTZ, 2 mg/kg CFZ, 3 mg/kg OBX, BTZ (2 mg/kg)–OBX (3 mg/kg) combination, and CFZ (2 mg/kg)–OBX (3 mg/kg) combination. The drug doses were chosen based on previous in vivo regimens used by others [27]. Treatments were given every 3 days for 21 days. As shown in Fig. 8a, b, BTZ or OBX single agents resulted in some level of growth inhibition. However, the addition of OBX significantly reduced the tumor size (42% reduction vs BTZ alone, $P = 0.0493$; 35% reduction vs CFZ alone, $P = 0.0349$). At the end of the experiment, we dissected the tumors from the animals and tried to determine the exact weights of the tumors in each group. We found that tumors from the combined treatment groups, BTZ–OBX and CFZ–OBX, weighed 64.7% ($P = 0.0108$) and 57.3% ($P = 0.0185$) less than the respective single agent treatment (Fig. 8c). The combination treatments did not appear to alter the weights of

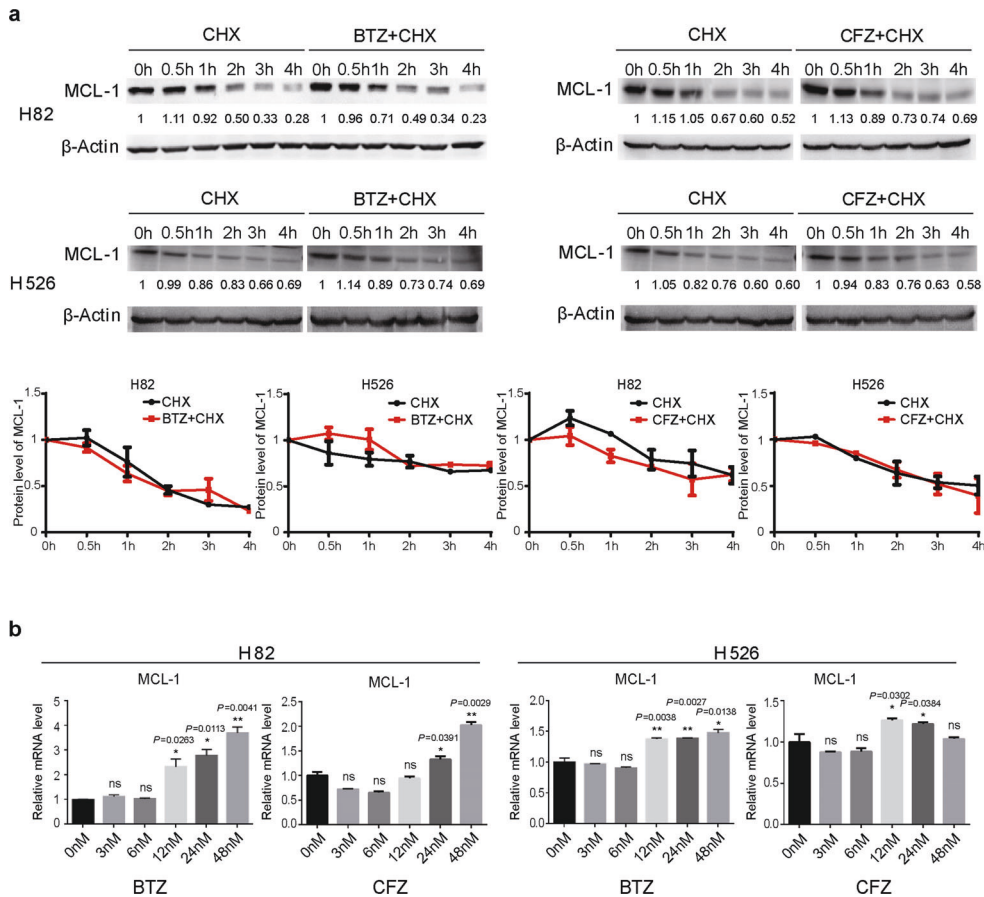


Fig. 5 BTZ and CFZ induced the transcription of MCL-1 rather than inhibiting its degradation. **a** The degradation of MCL-1 was not inhibited by BTZ or CFZ treatment. H82 and H526 cells were treated with 50 µg/mL CHX alone or combined with 12 nM BTZ/24 nM CFZ for 0, 0.5, 1, 2, 3, or 4 h. The expression of MCL-1 was detected by Western blotting. β-Actin was used as a loading control. The density of the bands was quantified and normalized to the respective β-Actin band intensity. The line graph presents the normalized densitometry data for MCL-1. **b** BTZ- and CFZ-induced MCL-1 mRNA levels in H82 and H526 cells. H526 and H82 cells were treated with DMSO or BTZ/CFZ for 24 h. The relative mRNA level of MCL-1 was determined by quantitative RT-PCR.

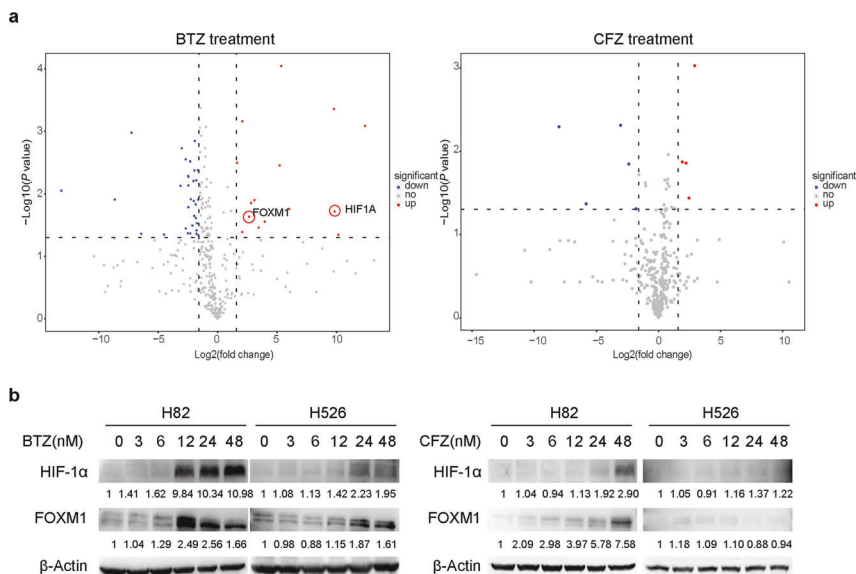


Fig. 6 Proteome-wide profiling analysis of activated transcription factors indicated that HIF-1α and FOXM1 were preferentially induced by BTZ treatment. **a** Volcano plots for different changed TFs after treatment with BTZ or CFZ. **b** Validation of HIF-1α and FOXM1 upregulation by BTZ/CFZ treatment in SCLC cells by Western blotting analysis. SCLC cells (H82 and H526 cells) were treated with DMSO control or different doses of BTZ/CFZ for 24 h. After treatment, HIF-1α and FOXM1 were detected by Western blotting. β-Actin was used as a loading control. The density of the bands was quantified and normalized to the respective β-Actin band intensity.

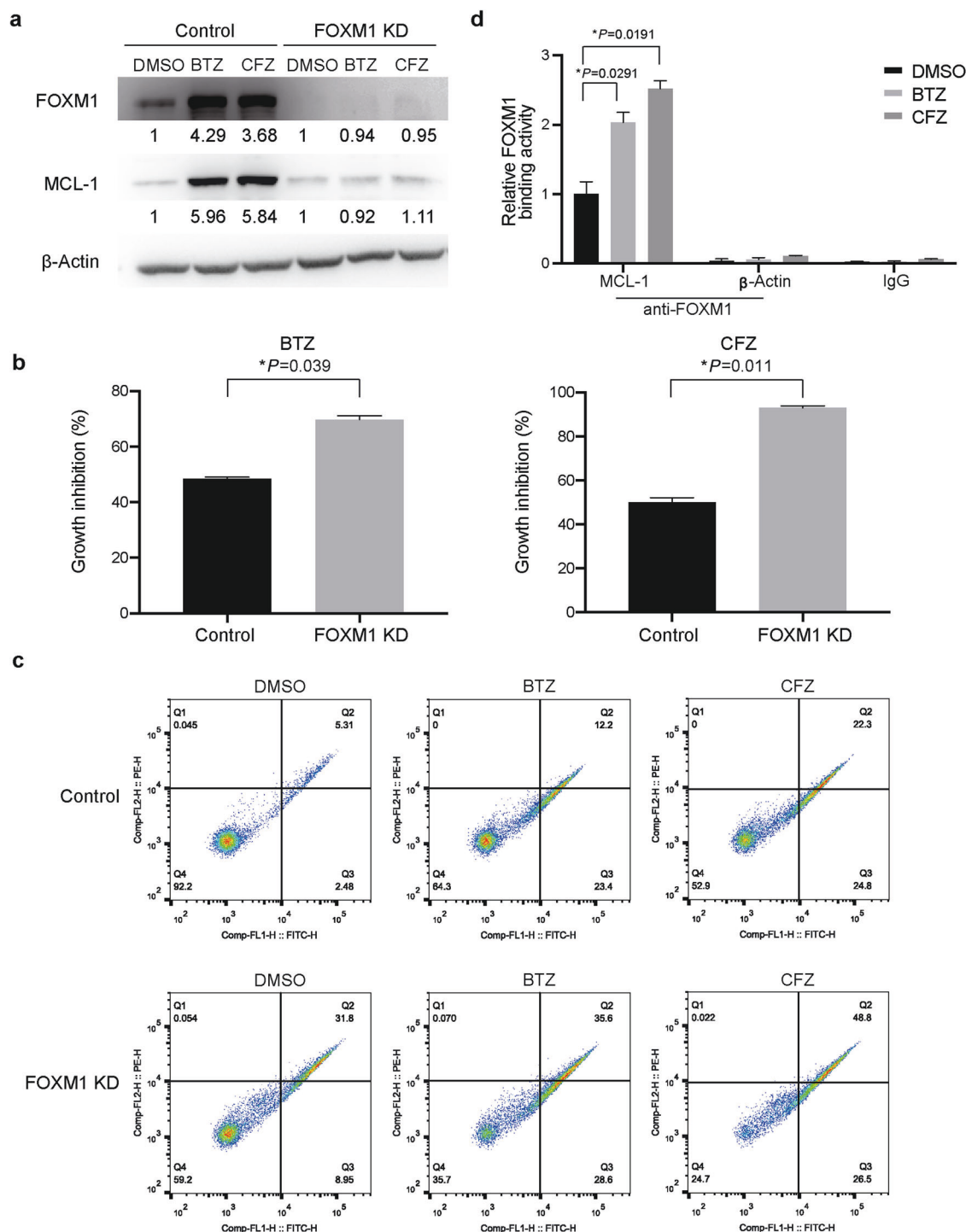


Fig. 7 FOXM1 mediated the upregulation of MCL-1 by BTZ and CFZ. **a** Knockdown of FOXM1 decreased the MCL-1 upregulation by BTZ and CFZ. H196 cells with stable expression of FOXM1 shRNA or control shRNA were treated with DMSO, BTZ (12 nM) or CFZ (48 nM) for 24 h, and then Western blotting was performed to detect the expression levels of FOXM1 and MCL-1. β-Actin was used as a loading control. The density of the bands was quantified and normalized to the respective β-Actin band intensity. **b** The inhibition of SCLC cell growth by BTZ or CFZ was significantly enhanced upon FOXM1 knockdown. H196 cells with stable expression of FOXM1 shRNA or control shRNA were treated with 12 nM BTZ or 1 nM CFZ for 72 h. The growth inhibition of cells was determined by the CellTiter-Glo Luminescent assay after treatment. **c** The cellular apoptosis induced by BTZ or CFZ was increased upon FOXM1 knockdown. H196 cells with stable expression of FOXM1 shRNA or control shRNA were treated with DMSO control, BTZ (12 nM), or CFZ (3 nM) for 24 h. After treatment, an Annexin V apoptotic assay was performed by flow cytometry. The percentage of apoptotic cells (Annexin V positive) is shown in regions Q2 and Q3. **d** The interaction of FOXM1 with the promoter region of MCL-1. H82 cells were treated with DMSO, BTZ (12 nM) or CFZ (48 nM) for 24 h, and the interaction of FOXM1 with the promoter region of MCL-1 was assessed by chromatin immunoprecipitation assay. The relative activity of FOXM1 binding to the MCL-1 or β-Actin promoter was detected by qPCR. Anti-normal mouse IgG was used as a negative control.

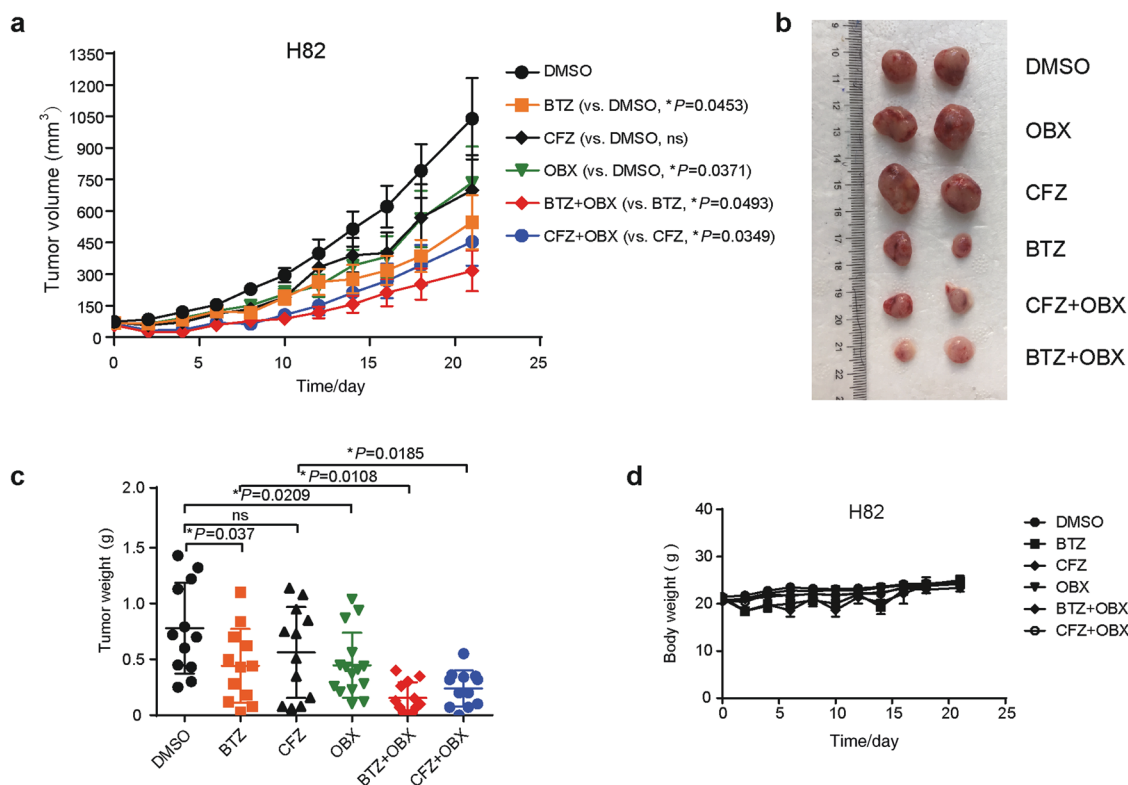


Fig. 8 OBX enhanced the antitumor activity of BTZ or CFZ in vivo. **a** Combination treatment with BTZ/CFZ and OBX leads to robust antitumor activity in SCLC xenografts. H82 xenografts were treated by intraperitoneal injection with DMSO control, BTZ (2 mg/kg), CFZ (2 mg/kg), OBX (3 mg/kg), the combination of BTZ (2 mg/kg) with OBX (3 mg/kg) or the combination of CFZ (2 mg/kg) with OBX (3 mg/kg) every 3 days. The tumor size was monitored by caliper measurements and calculated by the following formula: Volume = (length × width × width)/2. The mean tumor size ± SEM is shown. **b** Imaging of representative tumors from each group. The tumors were excised at the end of the experiment. The mean tumor weight ± SEM is shown. **c** The tumor weights in each group. The tumors were excised at the end of the experiment. The mean tumor weight ± SEM is shown. **d** There was no obvious difference in mouse weights from H82 xenografts during the course of treatment compared to the control group. Detection was conducted every 2 days from day 0 to the end of the experiment. The mean body weight ± SEM is shown.

the mice, indicating minimal toxicity of these combinations in vivo (Fig. 8d). Furthermore, we found that, by Ki-67 immunohistochemical staining, the tumors of the combination group displayed a statistically significant reduction in Ki-67 proliferation marker staining compared with single agents alone (BTZ–OBX 52.3% less than single BTZ treatment, $P < 0.0001$; CFZ–OBX 65.1% less than single CFZ treatment, $P < 0.0001$), demonstrating that these combinations could markedly halt SCLC tumor cell proliferation in vivo (Fig. 9a, b, Supplementary Fig. 4a). Apoptosis (cleaved-caspase 3 staining) was significantly increased in the tumors treated with the BTZ–OBX or CFZ–OBX combination (BTZ–OBX 5.3-fold more than single BTZ treatment, $P < 0.0001$; CFZ–OBX 1.5-fold more than single CFZ treatment, $P = 0.0018$) (Fig. 9c, Supplementary Fig. 4b). Our findings first demonstrated that proteasome inhibitors can be effective against SCLC in vivo when combined with OBX, which has anti-MCL-1 and apoptosis-inducing activities.

DISCUSSION

Proteasome inhibitors have an important role in cancer therapy, but drug resistance often develops and limits their clinical utility. In this study, we aimed to improve the antitumor activities of proteasome inhibitors in SCLC. Through proteomics analysis, our study identified an antiapoptosis protein, MCL-1, that was transcriptionally induced by BTZ and CFZ through FOXM1 upregulation in SCLC cells. The anticancer efficacy of BTZ and CFZ can be synergistically enhanced by OBX, an antagonist of MCL-1 in SCLC.

Our findings demonstrated for the first time that the antitumor activity of proteasome inhibitors can be enhanced when combined with OBX, an antagonist of MCL-1. OBX was developed as a pan-BCL-2 inhibitor that can displace Bak from MCL-1 or BCL-X_L [28]. Interestingly, in our study, we found that the combination of OBX effectively decreased the BTZ- or CFZ-induced expression of MCL-1. This might be a potential mechanism of BTZ/OBX or CFZ/OBX synergism against SCLC.

In SCLC, a phase II study of carboplatin and etoposide combined with OBX showed that OBX was well tolerated but failed to significantly improve patient survival [22]. Another phase I study of OBX plus topotecan also showed that OBX was safe and well tolerated [29]. Similarly, the clinical trials of BTZ or CFZ in SCLC indicated that the two FDA-approved drugs were well tolerated but lacked clinical efficacy. In our in vivo study, the two FDA-approved proteasome inhibitors demonstrated marked antitumor efficacies against SCLC when combined with OBX. Thus, combinations of proteasome inhibitors and OBX with acceptable toxicity profiles in humans could be readily amenable for SCLC patient treatment in future phase II clinical trials.

Our study demonstrated that MCL-1 was transcriptionally induced by BTZ and CFZ through FOXM1 upregulation. FOXM1 is a member of the Forkhead family of TFs and plays multiple roles in cell proliferation, cell cycle progression, invasion, and metastasis [30]. Hu et al. reported that MCL-1 was a target gene of FOXM1, and the expression of FOXM1/MCL-1 was coupled in gastric cancer, leading to resistance to chemotherapy [18]. MCL-1 is a short-lived protein whose level is tightly regulated by proteasome-mediated degradation [24]. Previous studies have indicated that

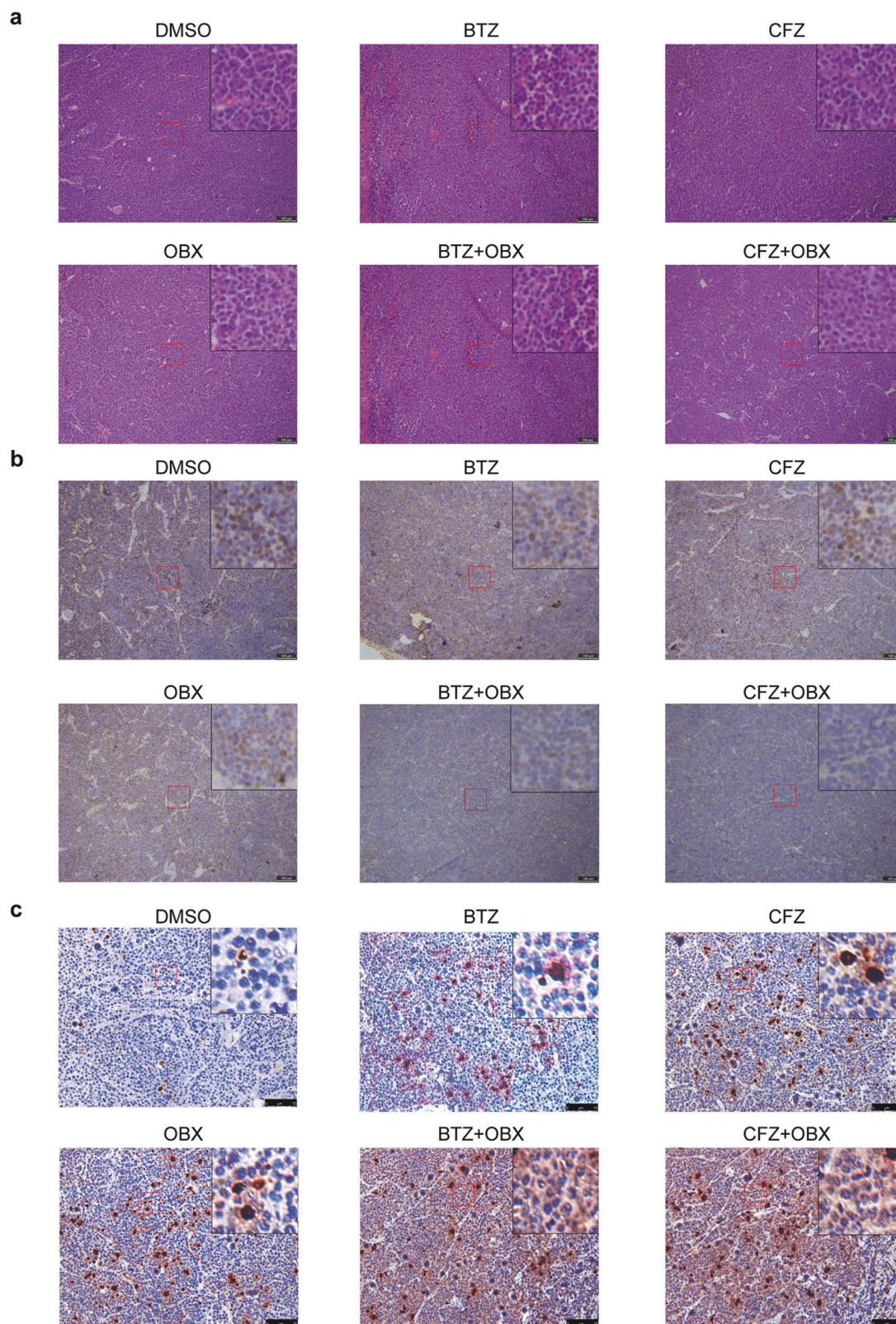


Fig. 9 Histologic analysis of tumors for cellular proliferation and apoptosis. **a** H&E staining of the SCLC xenografted tumors. Scale bars represent 100 μm . **b** Immunohistochemical detection of the proliferation marker Ki-67 in SCLC xenografted tumors. Scale bars represent 100 μm . **c** Immunohistochemical detection of the SCLC xenografted tumors for the apoptotic marker cleaved-caspase 3. Scale bars represent 75 μm . Small boxed areas were enlarged.

CFZ induced the accumulation of polyubiquitinated MCL-1 [31]. Hu et al. reported that BTZ induced the transcription of MCL-1 through the upregulation of activating transcription factor-4 in multiple myeloma [32]. In this study, we found for the first time that FOXM1 was induced by BTZ and CFZ, thereby leading to the transcriptional activation of MCL-1 in SCLC.

According to the proteomic data, some other proteins upregulated by BTZ and CFZ may be associated with SCLC resistance to proteasome inhibitors. Some of these proteins, such as UIMC1 and RAD18, are related to DNA damage repair. The activation of the DNA damage repair pathway enhances the ability of cells to recognize and repair DNA damage, which is associated with drug resistance [33]. UIMC1 was induced by BTZ (204-fold) and CFZ (1.2-fold). UIMC1 is responsible for the recruitment of the BRCA1 A complex (BRCA1, BARD1, BRCC36, Abraxas, and RAP80) to the sites of DNA damage [34]. RAD18 was induced by BTZ (39-fold) and CFZ (1.2-fold), and its high expression has been reported to mediate radiation resistance in glioma [35]. Therefore, the activation of the DNA damage repair pathway may be a mechanism of SCLC resistance to proteasome inhibitors.

DATA AVAILABILITY

Raw MS data were uploaded to iProX. These data can be accessed at the following url: <https://www.iprox.org/page/PSV023.html?url=1596784470810tGwJ> (keywords, sDU3).

ACKNOWLEDGEMENTS

This study was supported by the National Natural Science Foundation of China (Grant Numbers: 81672647, 81872438, 81502632, 81372214, and 81972191), Natural Science Foundation of Anhui Province (Grant Number: 1608085MH179), Science and Technology Major Project of Anhui Province (Grant Number: 18030801140) and 100-Talent Program of Chinese Academy of Sciences. A portion of this work was supported by the High Magnetic Field Laboratory of Anhui Province.

AUTHOR CONTRIBUTIONS

BH, WCL, and CD designed the study. YPY, BH, WHS, KD, and XLL performed the experiments. BH, YPY, WHS, HL, XTL, CD, and WCL analyzed and interpreted the data. YPY, BH and WHS wrote the manuscript. VWYL, WCL, and CD critically commented and edited the manuscript. All authors read and approved the final version of the manuscript.

ADDITIONAL INFORMATION

The online version of this article (<https://doi.org/10.1038/s41401-020-00544-w>) contains supplementary material, which is available to authorized users.

Competing interests: The authors declare no competing interests.

REFERENCES

- Manasanch EE, Orlowski RZ. Proteasome inhibitors in cancer therapy. *Nat Rev Clin Oncol.* 2017;14:417–33.
- Zhuang J, Shirazi F, Singh RK, Kuitse I, Wang H, Lee HC, et al. Ubiquitin-activating enzyme inhibition induces an unfolded protein response and overcomes drug resistance in myeloma. *Blood.* 2019;133:1572–84.
- Dou QP, Zonder JA. Overview of proteasome inhibitor-based anti-cancer therapies: perspective on bortezomib and second generation proteasome inhibitors versus future generation inhibitors of ubiquitin-proteasome system. *Curr Cancer Drug Targets.* 2014;14:517–36.
- Steele JM. Carfilzomib: a new proteasome inhibitor for relapsed or refractory multiple myeloma. *J Oncol Pharm Pr.* 2013;19:348–54.
- McBride A, Klaus JO, Stockerl-Goldstein K. Carfilzomib: a second-generation proteasome inhibitor for the treatment of multiple myeloma. *Am J Health Syst Pharm.* 2015;72:353–60.
- Tsakiri EN, Terpos E, Papanagnou ED, Kastritis E, Brioudes V, Halabalaki M, et al. Milder degenerative effects of Carfilzomib vs. Bortezomib in the *Drosophila* model: a link to clinical adverse events. *Sci Rep.* 2017;7:17802.

- Okazuka K, Ishida T. Proteasome inhibitors for multiple myeloma. *Jpn J Clin Oncol.* 2018;48:785–93.
- Byers LA, Rudin CM. Small cell lung cancer: where do we go from here? *Cancer.* 2015;121:664–72.
- Waqar SN, Morgensztern D. Treatment advances in small cell lung cancer (SCLC). *Pharm Ther.* 2017;180:16–23.
- Morabito A, Carillio G, Daniele G, Piccirillo MC, Montanino A, Costanzo R, et al. Treatment of small cell lung cancer. *Crit Rev Oncol Hematol.* 2014;91:257–70.
- Lara PN Jr, Chansky K, Davies AM, Franklin WA, Gumerlock PH, Guaglianone PP, et al. Bortezomib (PS-341) in relapsed or refractory extensive stage small cell lung cancer: a Southwest Oncology Group phase II trial (S0327). *J Thorac Oncol.* 2006;1:996–1001.
- Baker AF, Hanke NT, Sands BJ, Carbajal L, Anderl JL, Garland LL. Carfilzomib demonstrates broad anti-tumor activity in pre-clinical non-small cell and small cell lung cancer models. *J Exp Clin Cancer Res.* 2014;33:111.
- Arnold SM, Chansky K, Leggas M, Thompson MA, Villano JL, Hamm J, et al. Phase 1b trial of proteasome inhibitor carfilzomib with irinotecan in lung cancer and other irinotecan-sensitive malignancies that have progressed on prior therapy (Onyx IST reference number: CAR-IST-553). *Investig N. Drugs.* 2017;35:608–15.
- Shi W, Li K, Song L, Liu M, Wang Y, Liu W, et al. Transcription factor response elements on tip: a sensitive approach for large-scale endogenous transcription factor quantitative identification. *Anal Chem.* 2016;88:11990–4.
- Ding C, Chan DW, Liu W, Liu M, Li D, Song L, et al. Proteome-wide profiling of activated transcription factors with a concatenated tandem array of transcription factor response elements. *Proc Natl Acad Sci U S A.* 2013;110:6771–6.
- Feng J, Ding C, Qiu N, Ni X, Zhan D, Liu W, et al. Firmiana: towards a one-stop proteomic cloud platform for data processing and analysis. *Nat Biotechnol.* 2017;35:409–12.
- Wang H, Hong B, Li X, Deng K, Li H, Yan Lui VW, et al. JQ1 synergizes with the Bcl-2 inhibitor ABT-263 against MYCN-amplified small cell lung cancer. *Oncotarget.* 2017;8:86312–24.
- Hu CJ, Wang B, Tang B, Chen BJ, Xiao YF, Qin Y, et al. The FOXM1-induced resistance to oxaliplatin is partially mediated by its novel target gene Mcl-1 in gastric cancer cells. *Biochim Biophys Acta.* 2015;1849:290–9.
- Lodhi N, Tulin AV. PARP1 genomics: chromatin immunoprecipitation approach using anti-PARP1 antibody (ChIP and ChIP-seq). *Methods Mol Biol.* 2011;780:191–208.
- Chou TC. Drug combination studies and their synergy quantification using the Chou-Talalay method. *Cancer Res.* 2010;70:440–6.
- Hong B, Wang H, Deng K, Wang W, Dai H, Yan Lui VW, et al. Combination treatment of RAD001 and BEZ235 exhibits synergistic antitumor activity via down-regulation of p-4E-BP1/Mcl-1 in small cell lung cancer. *Oncotarget.* 2017;8:106486–98.
- Langer CJ, Albert I, Ross HJ, Kovacs P, Blakely LJ, Pajkos G, et al. Randomized phase II study of carboplatin and etoposide with or without obatoclax mesylate in extensive-stage small cell lung cancer. *Lung Cancer.* 2014;85:420–8.
- Chiappori AA, Schreeder MT, Moezi MM, Stephenson JJ, Blakely J, Salgia R, et al. A phase I trial of pan-Bcl-2 antagonist obatoclax administered as a 3-h or a 24-h infusion in combination with carboplatin and etoposide in patients with extensive-stage small cell lung cancer. *Br J Cancer.* 2012;106:839–45.
- Mojca B, Lassot I, Desagher S. Mcl-1 ubiquitination: unique regulation of an essential survival protein. *Cells.* 2014;3:418–37.
- Harrison LR, Micha D, Brandenburg M, Simpson KL, Morrow CJ, Denny O, et al. Hypoxic human cancer cells are sensitized to BH-3 mimetic-induced apoptosis via downregulation of the Bcl-2 protein Mcl-1. *J Clin Invest.* 2011;121:1075–87.
- Bhattacharyya A, Chattopadhyay R, Hall EH, Mebrahtu ST, Ernst PB, Crowe SE. Mechanism of hypoxia-inducible factor 1 alpha-mediated Mcl1 regulation in *Helicobacter pylori*-infected human gastric epithelium. *Am J Physiol Gastrointest Liver Physiol.* 2010;299:G1177–86.
- Dasmahapatra G, Lembersky D, Son MP, Patel H, Peterson D, Attkisson E, et al. Obatoclax interacts synergistically with the irreversible proteasome inhibitor carfilzomib in GC- and ABC-DLBCL cells in vitro and in vivo. *Mol Cancer Ther.* 2012;11:1122–32.
- Nguyen M, Marcellus RC, Roulston A, Watson M, Serfass L, Murthy Madiraju SR, et al. Small molecule obatoclax (GX15-070) antagonizes MCL-1 and overcomes MCL-1-mediated resistance to apoptosis. *Proc Natl Acad Sci U S A.* 2007;104:19512–7.
- Paik PK, Rudin CM, Brown A, Rizvi NA, Takebe N, Travis W, et al. A phase I study of obatoclax mesylate, a Bcl-2 antagonist, plus topotecan in solid tumor malignancies. *Cancer Chemother Pharmacol.* 2010;66:1079–85.
- Nandi D, Cheema PS, Jaiswal N, Nag A. FoxM1: repurposing an oncogene as a biomarker. *Semin Cancer Biol.* 2018;52:74–84.
- Lamothe B, Wierda WG, Keating MJ, Gandhi V. Carfilzomib triggers cell death in chronic lymphocytic leukemia by inducing proapoptotic and endoplasmic reticulum stress responses. *Clin Cancer Res.* 2016;22:4712–26.

32. Hu J, Dang N, Menu E, De Bruyne E, Xu D, Van Camp B, et al. Activation of ATF4 mediates unwanted Mcl-1 accumulation by proteasome inhibition. *Blood*. 2012;119:826–37.
33. Goldstein M, Kastan MB. The DNA damage response: implications for tumor responses to radiation and chemotherapy. *Annu Rev Med*. 2015;66:129–43.
34. Jin F, Ma T, Guan H, Yang ZH, Liu XD, Wang Y, et al. Inhibitory effect of uranyl nitrate on DNA double-strand break repair by depression of a set of proteins in the homologous recombination pathway. *Toxicol Res*. 2017;6:711–8.
35. Wu B, Wang H, Zhang L, Sun C, Li H, Jiang C, et al. High expression of RAD18 in glioma induces radiotherapy resistance via down-regulating P53 expression. *Biomed Pharmacother*. 2019;112:108555.